

Noninvasive Blood Glucose Measurement Using Live Video by Smartphone

Jannatun Sumaiya

Department of Electrical and
Electronic Engineering
Khulna University of Engineering
& Technology
Khulna 9203, Bangladesh
jannatunsumaiya@gmail.com

Md. Rakibul Hasan

Department of Electrical and
Electronic Engineering
Khulna University of Engineering
& Technology
Khulna 9203, Bangladesh
rakibul.eeekuet@gmail.com

Eklas Hossain

Department of Electrical Engineering
and Renewable Energy
Oregon Institute of Technology
OR 97601, USA
eklas.hossain@oit.edu

Abstract—In this paper, we have presented the noninvasive monitoring of blood glucose concentration that was performed by using the smartphones camera, different lighting sources, and the near infra-spectroscopy used by transmission photoplethysmography (PPG). The system implementation was associated with getting the PPG signal at the near infra wavelengths of 850 nm and 1070 nm. The processing of the photoplethysmography (PPG) signal was carried out with the Linear Regression (LR), Support Vector Regression (SVR), Deep Neural Network (DNN), and Random Forest Regression (RFR) for estimating the glucose level in the blood. We have collected three sets of data and analyzed them using the Python programming language to find out the relation between blood glucose concentration and photoplethysmography (PPG). The predicted glucose level was 4.7 mg/dl with respect to 5 mg/dl.

Index Terms—Blood glucose, Noninvasive, Near infrared absorbance, Photoplethysmography (PPG)

I. INTRODUCTION

More than 400 million grown-ups experience diabetes mellitus due to the disturbance of producing insulin to balance blood glucose level. People who suffer from diabetes have long term dangerous effects that lead to blindness, damaged nerves, and kidneys, and other diseases like the risk of heart stroke are also increased [1]. The patients of diabetic require blood glucose monitoring more frequently. Nowadays, the invasive technique is available for blood glucose for self-monitoring that is painful and sometimes expensive. It also requires a new strip and drawing of blood from the finger that involves the risk of spreading infection. Because of these undesirable effects of the invasive methods, including associated additional cost, many researchers proposed some non-invasive techniques, which are becoming popular day by day [2]–[5].

There are two types of diabetes known as Type I and Type II. Type I is found in teenagers, which is known as Juvenile, and it is 10% of the world's total diabetic patients. Type II is found in mature persons, and it is the most common diabetes. Observation of the noninvasive glucose can be of two types, which are optical analysis and non-optical analysis [6]. The classifications of the optical inspection are near-infrared spectroscopy, mid-infrared spectroscopy, Raman spectroscopy, optical coherence tomography, photoacoustic spectroscopy,

and so on. The classifications of non-optical inspection are Conservation Of Energy Metabolism (COEM) and Dielectric Spectroscopy (DS) or Bio-Impedance Spectroscopy (BIS), and so forth [7]. The noninvasive measurement of blood glucose, as used by most of the researchers, is the PPG signal to reduce pain during blood extraction and insulin injection. In this paper, we have used various methods like infrared and PPG signals for the detection of glucose in the blood [8], [9]. The measurement of the blood glucose level by noninvasive technique develops a pain-free glucose monitoring system, and this is the only way without pain. The direct measurement of body tissues, for example, the skin, tongue, aqueous humor of the eyes, and mucosa can be used for the measurement of blood glucose level [10]. The proposed method makes the difference in the measurement of different blood glucose level using the absorbance principle. Firstly, we generated an image, and secondly, that image was cropped by 600 frames, and then, a PPG signal was generated to extract the three best PPG waves. After that, the fundamental features were extracted from the best three PPG waves, and the data were trained through different machine learning models to find out the best model to predict blood glucose level non-invasively.

In this paper, section II consists of the description of the proposed system. The methodologies used in this system are discussed in section III. A system overview is shown at section IV. The result obtained from the proposed system is analyzed and discussed in section V. Finally, the study has been justified and concluded in section VI.

II. SYSTEM DESCRIPTION

A. Equipment Configuration

The proposed blood glucose measurement system requires a simple data collection kit and a smartphone, as illustrated in Fig. 1. The data collection kit for this purpose was a high-intense LED light. As shown in Fig. 1a to Fig. 1c, the finger needs to be kept over the kit and then the LED should be turned on. After that, the setup is ready for collecting video by using a smartphone camera. In Fig. 1d, the procedure of collecting video by using only a smartphone has been illustrated. In this case, the finger should be placed over the

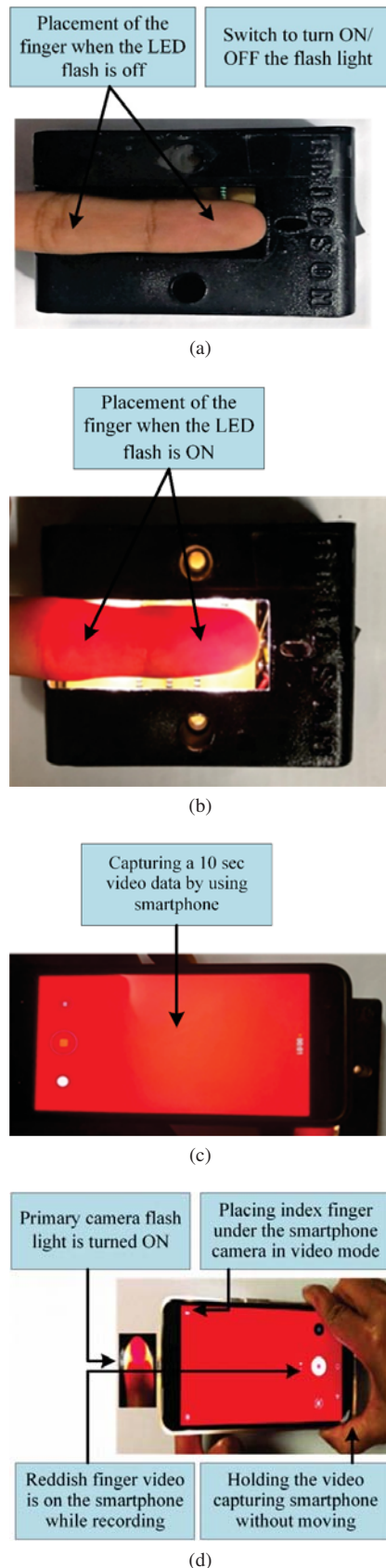


Fig. 1. Video data collection: (a) Index finger on the collection kit while the kit flashlight is off. (b) Index finger on the collection kit while the kit flashlight is on. (c) Taking the video data by a smartphone camera. (d) Video data collection without any external onboard LED.

smartphone's primary camera and LED flashlight, and then, the video should be recorded. This method is convenient because it does not require any external data collection kit, although, placing a finger directly over the smartphone camera and LED flash light could damage the smartphone camera.

B. Data Collection

At the time of collecting data, we kept in mind that the finger was cleaned and dry, no nail polish was allowed, and there was no infection in the finger. Then the finger was put in the LED board, as showed in Fig. 1a to Fig. 1c, and collected data, as shown in Fig. 1d. We collected age, gender, gold standard Hb, Glucose, and HbA1c from the clinic with permission from concerned authority. We followed the same procedure for each LED board.

C. Data Preprocessing

For each lighting condition, we took 10+ sec (60 fps) videos by Google Pixel-2 smartphone, and then only 600 frames were extracted for each video. We have applied bandpass filter on the red channel with frequency per second (fps)=60, minimum blood pulse per minute (BPM L) = 40, maximum blood pulse per minute (BPM H) = 500, and order = 2. We took a reverse bandpass filter that is similar to the PPG wave as well as only the three best PPG waves, which has the best three highest positive peaks. Fig. 2 demonstrates the channel classification process from the raw video.

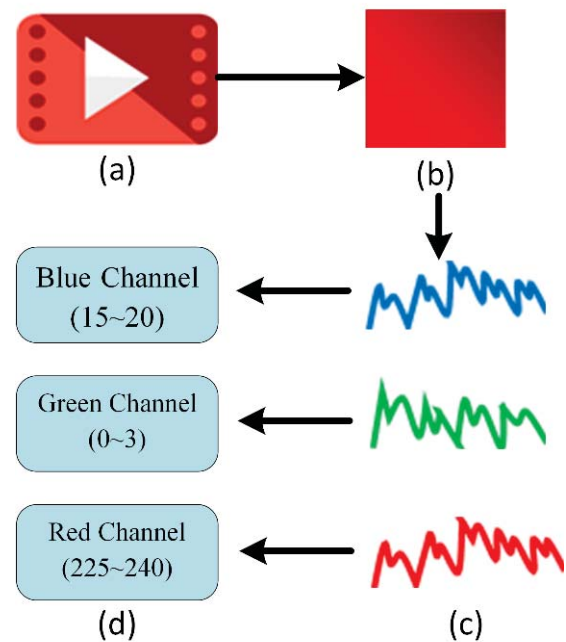


Fig. 2. (a) Raw video that was taken with Google pixel-2 smart-phone. (b) Extract frames: Cropped frame (500x500) pixel from right to left section of extracted frame (1920x1080) pixel. (c) Time series plot of average intensity for 3 channels from all cropped frames. (d) Intensity range classification.

D. Feature Extraction and Selection

For feature extraction that is required for training the machine learning models, the time series of only the red channel has been taken and PPG waves have been derived as shown in Fig. 3.

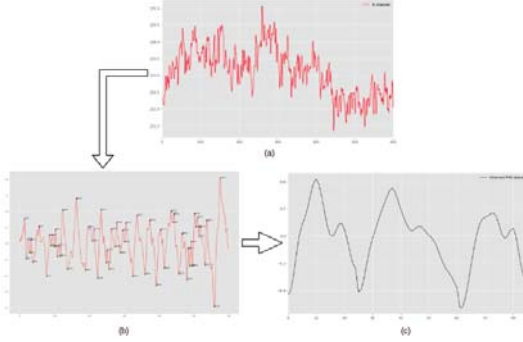


Fig. 3. (a) Time series of the red channel, (b) PPG waves, (c) Selected best three PPG waves. For feature extraction, we generated Photoplethysmography (PPG) for each subject's fingertip video.

The blood movement is reflected, but the PPG signal goes from the heart (center) to the fingertips (end) in the blood vessels in a wave-like motion [7] as demonstrated by Fig. 4. The wave contour is simpler as compared to the PPG signal. The analysis and investigation are quite impossible due to the difficulty in detecting changes in the phase of the inflections in the original fingertip PPG of Fig. 4.

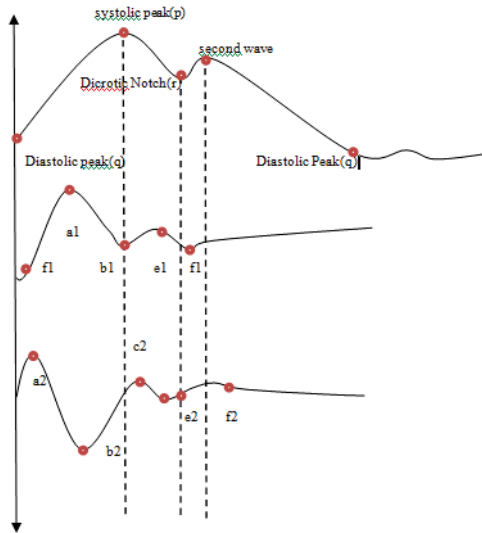


Fig. 4. Original measured fingertip PPG signal, after first derivation of PPG wave, and second derivation of PPG wave, respectively.

In Fig. 4, first and second derivatives of the raw PPG signal are shown, which helps to find a better interpretation of the signal, and it facilitates more accurate recognition of inflection points.

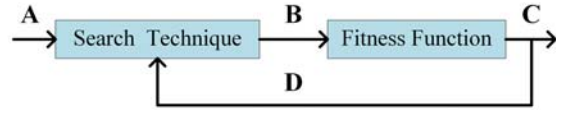


Fig. 5. Block diagram of features selection process using Genetic Algorithm (GA). Here, A = Original Feature Set, B = Feature Subset, C = Optimal Feature Subset, and D = Goodness of Fit.

The feature selection process has been done by using genetic algorithm as illustrated in Fig. 5. It is a stochastic algorithm and can pull out good solutions trapped in a local solution [11].

III. METHODOLOGY

A. Linear Regression (LR)

Linear Regression (LR) is one of the simplest and popular machine learning techniques for data analysis. Equation (1) demonstrates the theorem behind every linear regression model [12].

$$b(a, c) = c_0 + c_1 a_1 + c_2 a_2 + \dots + c_n a_n \quad (1)$$

where, c_0 = interception, $c = (c_1, c_2, \dots, c_n)$ = learning coefficients, $a = (a_1, a_2, a_3, \dots, a_n)$ = input data, and b = predicted value. The optimization or loss function, which represents the minimum normalized square error between the actual value and the predicted value is shown in (2).

$$\min_c = \|A_c - b\|^2 \quad (2)$$

where, A_c represents the actual observable value and b is the predicted value.

B. Support Vector Regression (SVR)

In this technique, the datasets are considered in high dimensional feature space, and it finds out the maximum margin that is called the critical points of the dataset in Support Vector Regression (SVR). Equation (3) represents the optimization function [13].

$$\begin{aligned} \min \frac{1}{2} \|c\|^2 \\ b_i - (c, a_i) - c_o \leq \epsilon \\ (c, a_i) + c_o - b_i \leq \epsilon \end{aligned} \quad (3)$$

where, ϵ is the deviation or error between the observed actual value and the predicted value.

C. Random Forest Regression (RFR)

Random Forest Regression (RFR) is one of the supervised Regression techniques. The classification of RFR is an ensemble method, and it can be thought of as a form of the nearest neighbor predictor. There are four basic steps of Random Forest Techniques. Firstly, we pick a random K data point from the training set. Secondly, we build a decision tree that is associated with these K data points. Thirdly, we choose the number of N trees for trees that are formed and repeat the first and second steps. Finally, new data is assigned to the category, and the vote for each predicted outcome formed from the decision trees are calculated. The Majority vote decides the final outcome of the random forest algorithm.

D. Deep Neural Network (DNN)

This machine learning method is based on learning data representations, which is called deep learning, and it is a part of a broader family. Two major techniques of supervised learning are classification and regression. Regression models have a dense layer at the end with a single output having no nonlinear activation function. Also, we can say that the activation function is linear, as shown in (4). For hidden layers, the most popular activation function is the rectified linear unit (ReLU), which is shown in (5). We have used Mean Absolute Error (MAE) as the loss function.

$$f(a) = a; a = (-, +) \quad (4)$$

$$R(z) = \max(0, z) \quad (5)$$

where, z represents the input value. If the value of z becomes less than zero, the output of this activation function will be zero. On the contrary, if the value of z becomes positive, the ReLU function returns the input value as output.

E. K-fold Cross-Validation Method

The K-fold cross-validation is a well-known method for evaluating the performance of different machine learning models for a limited amount of data. Fig. 6 describes the 10-fold cross-validation method. This method is useful specifically for smaller datasets. In this method, the dataset is shuffled randomly. Then the dataset is split into K groups. One group is used as a test dataset, while the others are used as a training dataset. After that, the average performance at all folds is used to evaluate the performance of the respective machine learning models. Here, the value of K is taken as 10, as it is the most commonly used [14], [15]. In this way, we have evaluated the performance of our machine learning models.

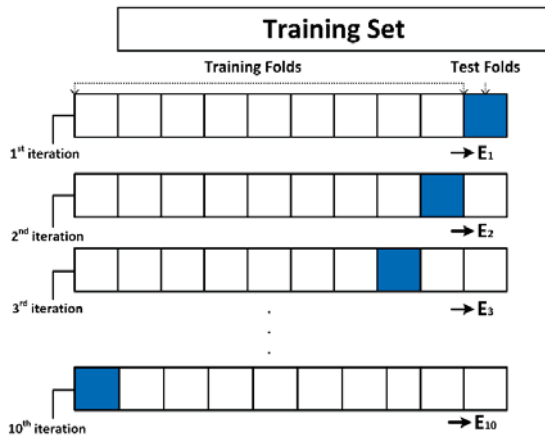


Fig. 6. Procedure of K-fold ($K = 10$) cross validation. Here, the dataset is randomly split into 10 different groups, and each group is tested against other groups of data.

IV. SYSTEM OVERVIEW

Fig. 7 shows the system overview of the proposed noninvasive blood glucose measurement system. At first, a short video of the blood was recorded from the finger through a

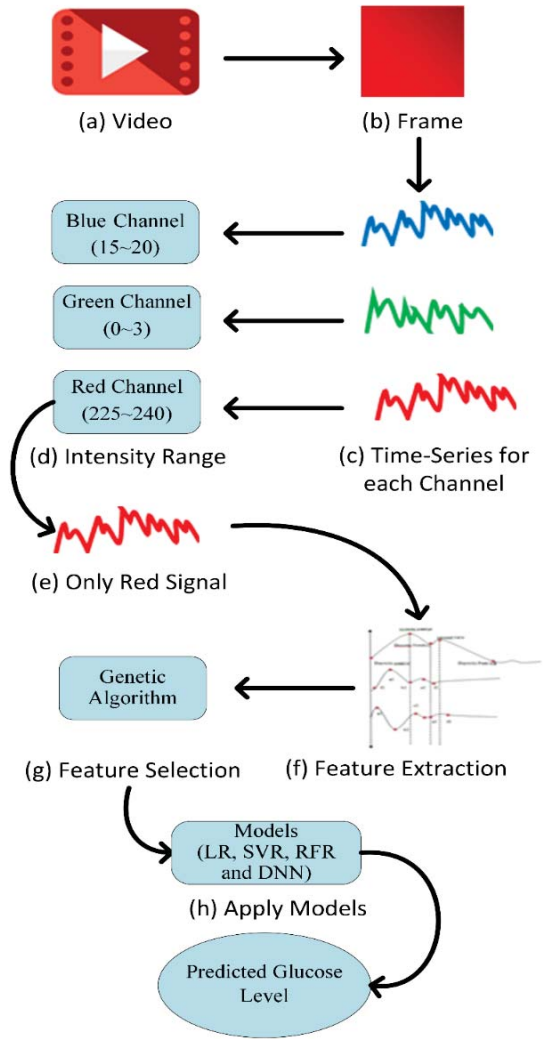


Fig. 7. The overall flowchart of the proposed noninvasive blood glucose measurement system. The total process includes: (a) Video recording, (b) Frame extraction, (c) Time series of signal, (d) Intensity range classification, (e) Channel separation, (f) PPG derivation from red channel time series, (g) Feature selection, and (h) Training models.

smartphone camera with a proper LED setup. Then each frame is captured from the video. The frames were divided into three channels—blue, green, and red. Then, only the time series of the red channel was taken. From the time series, PPG signals were derived. The fundamental features were extracted from the best PPG signals. Features were selected by using the genetic algorithm. Then different machine learning models have been applied to the data. After that, the prediction of blood glucose level has been achieved. Kfold cross-validation method has been used to analyze and validate each training model.

V. RESULT ANALYSIS AND DISCUSSION

As discussed in section III, linear regression, support vector regression, random forest regression, and deep neural network models have been used to train the collected dataset to predict the blood glucose level in the proposed noninvasive blood

glucose measurement system. We have observed a variation in the performance for different training models.

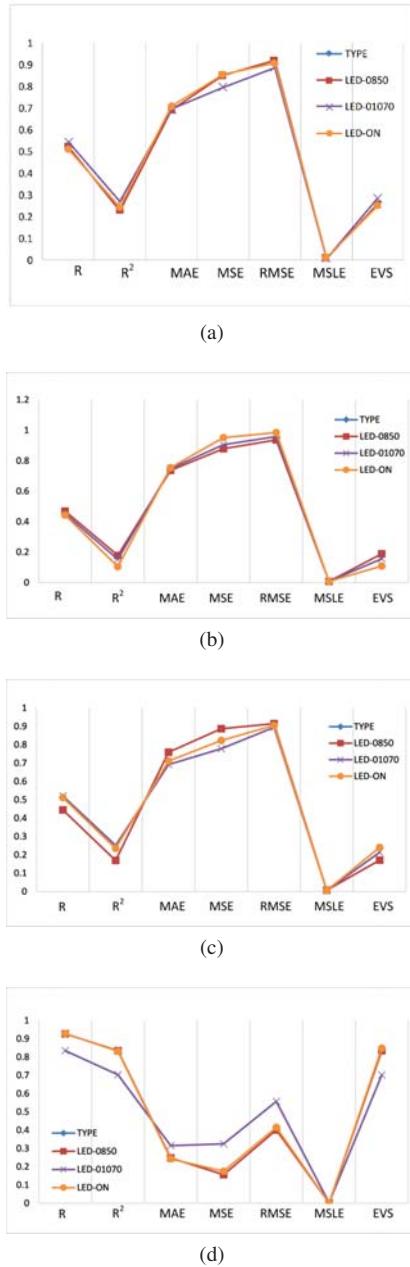


Fig. 8. Error analysis of (a) Linear regression, (b) SVR, (c) Random forest regression, and (d) DNN method for three different types of LEDs. Among these methods, the DNN method yields comparatively less error.

We have shown the Correlation Coefficient (R), Correlation of Determination (R^2), Mean Absolute Error (MAE), Root Mean Squared Error (RMSE), Mean Squared Logarithmic Error (MSLE), and Enumerator Variances (EVS) in Fig. 8 for four different training models in three different LED conditions. Among these models, the DNN model yielded lower level of MAE, MSE, RMSE, and MSLE, which denotes the best model. Also, the performance of LED-0850 was better in most cases, although, for random forest regression, the best performance came for LED-01070.

TABLE I
PERFORMANCE OF LINEAR REGRESSION ON DIFFERENT LEDs

LED Type	R	R^2	MAE	MSE	RMSE	MSLE	EVS
LED-0850	0.523	0.227	0.69	0.85	0.92	0.007	0.254
LED-01070	0.543	0.27	0.694	0.797	0.887	0.007	0.283
LED-ON	0.509	0.242	0.708	0.855	0.906	0.008	0.249

TABLE II
PERFORMANCE OF SUPPORT VECTOR REGRESSION ON DIFFERENT LEDs

LED Type	R	R^2	MAE	MSE	RMSE	MSLE	EVS
LED-0850	0.469	0.178	0.737	0.879	0.937	0.008	0.189
LED-01070	0.452	0.153	0.749	0.905	0.959	0.008	0.157
LED-ON	0.443	0.105	0.755	0.952	0.985	0.008	0.109

TABLE III
PERFORMANCE OF RANDOM FOREST REGRESSION ON DIFFERENT LEDs

LED Type	R	R^2	MAE	MSE	RMSE	MSLE	EVS
LED-0850	0.445	0.169	0.759	0.887	0.915	0.007	0.171
LED-01070	0.521	0.251	0.692	0.778	0.895	0.006	0.213
LED-ON	0.512	0.235	0.711	0.823	0.905	0.006	0.24

TABLE IV
PERFORMANCE OF DEEP NEURAL NETWORK ON DIFFERENT LEDs

LED Type	R	R^2	MAE	MSE	RMSE	MSLE	EVS
LED-0850	0.927	0.835	0.248	0.156	0.401	0.002	0.835
LED-01070	0.835	0.703	0.315	0.325	0.557	0.003	0.702
LED-ON	0.929	0.832	0.243	0.175	0.415	0.002	0.848

The values regarding the performance of each of these models have been tabulated in Table I to Table IV. The combination of LED-0850 with the Deep Neural Network model gave the best performance where the Correlation Coefficient (R) is 0.927, Correlation of Determination (R^2) is 0.835, and Mean Absolute Error (MAE) is 0.248 that is more than enough for day-to-day monitoring of blood glucose level.

VI. CONCLUSION

Regular monitoring of blood hemoglobin level is essential to determine glucose concentration in the blood. The glucose test is generally advised during a general health examination or when a person has signs and symptoms of a condition affecting red blood cells such as anemia or polycythemia. This paper presents a new way of regular monitoring of blood glucose

level that is essential to determine glucose concentration in the blood. The blood glucose test is a frequent health examination mostly necessary for elderly persons. The revelation of the analysis is the short-comings of invasive and minimally invasive methods and also the necessity of the increment of the noninvasive method that requires significant improvement to replace the conventional blood glucose monitoring devices. It gives another advantage of possibly avoiding the risk of the spread of infection among others as well. Four machine learning algorithms have been used in this work, and those four methods are briefly described in this paper. Among these methods, the best result came for the Deep Neural Network than other machine learning models, and we have got the best result on LED-0850. This paper reveals some new exploration of how to get data more simply and in a more efficient way, how to preprocess these data, and finally, with the help of an appropriate model, the blood glucose level is determined. As a future scope, a mobile application might be developed that would help the user to collect their data more efficiently.

REFERENCES

- [1] R. A. Meyers, Ed., *Encyclopedia of Analytical Chemistry*. Wiley, September 2006.
- [2] V. P. Rachim and W.-Y. Chung, "Wearable-band type visible-near infrared optical biosensor for non-invasive blood glucose monitoring," *Sensors and Actuators B: Chemical*, vol. 286, pp. 173–180, 2019.
- [3] A. Hina, H. Nadeem, and W. Saadeh, "A single led photoplethysmography-based noninvasive glucose monitoring prototype system," in *2019 IEEE International Symposium on Circuits and Systems (ISCAS)*, May 2019, pp. 1–5.
- [4] Y. Liu, M. Xia, Z. Nie, J. Li, Y. Zeng, and L. Wang, "In vivo wearable non-invasive glucose monitoring based on dielectric spectroscopy," in *2016 IEEE 13th International Conference on Signal Processing (ICSP)*. IEEE, 2016, pp. 1388–1391.
- [5] J. Kraitl, U. Timm, E. Lewis, and H. Ewald, "Optical sensor technology for a noninvasive continuous monitoring of blood components," in *Optical Diagnostics and Sensing X: Toward Point-of-Care Diagnostics*, vol. 7572. International Society for Optics and Photonics, 2010, p. 757209.
- [6] E. Vezouviou and C. R. Lowe, "A near infrared holographic glucose sensor," *Biosensors and Bioelectronics*, vol. 68, pp. 371–381, June 2015.
- [7] M. N. Anas and P. K. Lim, "A bio-impedance approach," in *2013 IEEE International Conference on Smart Instrumentation, Measurement and Applications (ICSIMA)*. IEEE, November 2013, pp. 1–5.
- [8] S. K. Vashist, "Non-invasive glucose monitoring technology in diabetes management: A review," *Analytica Chimica Acta*, vol. 750, pp. 16–27, 2012, 750th Anniversary Volume.
- [9] A. Duncan, J. Hannigan, S. S. Freeborn, P. W. H. Rae, B. McIver, F. Greig, E. M. Johnston, D. T. Binnie, and H. A. MacKenzie, "A portable non-invasive blood glucose monitor," in *Proceedings of the International Solid-State Sensors and Actuators Conference - TRANSDUCERS '95*, vol. 2, June 1995, pp. 455–458.
- [10] W.-C. Shih, K. L. Bechtel, and M. V. Rebec, "Noninvasive glucose sensing by transcutaneous Raman spectroscopy," *Journal of Biomedical Optics*, vol. 20, no. 5, pp. 1–5, 2015.
- [11] S. Mirjalili, "Evolutionary algorithms and neural networks," *Studies in Computational Intelligence*, 2019.
- [12] I. Guyon and A. Elisseeff, "An introduction to variable and feature selection," *Journal of machine learning research*, vol. 3, pp. 1157–1182, March 2003.
- [13] L. Wang, E. Pickwell-MacPherson, Y. Liang, and Y. T. Zhang, "Noninvasive cardiac output estimation using a novel photoplethysmogram index," in *2009 Annual International Conference of the IEEE Engineering in Medicine and Biology Society*. IEEE, 2009, pp. 1746–1749.
- [14] J. Brownlee, "A gentle introduction to k-fold cross-validation," *Machine Learning Mastery*, vol. 2019, 2018.
- [15] T. Fushiki, "Estimation of prediction error by using k-fold cross-validation," *Statistics and Computing*, vol. 21, no. 2, pp. 137–146, 2011.